EUROPEAN ORGANIZATION FOR NUCLEAR RESEARCH

CERN/SPSC 84-30
SPSC/P93 Add.2
May 15th 1984

PROPOSAL TO IMPROVE THE PERFORMANCE OF THE UA2 DETECTOR

The UA2 Collaboration

Bern - CERN - Orsay (LAL) - Pavia - Pisa Collaboration

1. INTRODUCTION

The UA2 experiment was approved by the Research Board on December 14th 1978, took its first data in November 1981, as soon as $\bar{p}p$ collisions took place, and has been operating smoothly since then. The very successful performance of the $Sp\bar{p}S$ collider has given us the opportunity to collect a rich harvest of data during this period. Their analysis has resulted in a number of observations and measurements which have a major impact on our understanding of nature :

i) the observation of two-jet dominance in large transverse energy final states [1], measurements of the inclusive jet production cross-section [1,2], and a study of jet production and fragmentation mechanisms [3],

ii) the observation of massive electron-neutrino pairs, providing evidence for the existence of the charged W bosons [4,5,6].

iii) the observation of massive electron pairs, providing evidence for the existence of the neutral Z^0 boson [6,7].

These results answer the questions which motivated the construction of UA2 and are in line with the predictions of the QCD and $SU(2)\otimes U(1)$ models of strong and electroweak interactions.

In addition unexpected observations have been made, which may suggest the existence of new phenomena : in particular the observations by UA2 [6,7], and UA1 [8] of $Z^0 \rightarrow e^+e^-\gamma$ decays, by UA2 [9] of electrons produced in association with hard jets and large missing transverse momentum, and by UA1 [10] of events with large missing transverse energy accompanied by a jet or a photon. The coming data taking periods of Autumn 1984 and 1985 will help to place these results on firmer ground. Then, after a long shut-down in 1986, the $Sp\bar{p}S$ collider will resume operation with a substantially higher luminosity than presently available. The recently approved Antiproton Collector (ACOL) should allow for a total integrated luminosity of nearly 10 pb^{-1} by the end of 1989. In order to make the best use of the increased luminosity in terms of physics results the performance of the present UA2 detector has to be simultaneously improved. In the present document we propose a number of modifications which we consider necessary to upgrade the UA2 apparatus to a level matching that of the improved Collider. In making our choices we have taken into account the limitations of the present design, considerations of competitivity with UA1 and with the TEV 1 programme, constraints of time table and the availability of manpower and money resources. In the next Section we present some general considerations along these lines. Section 3 is devoted to a description of the proposed calorimeter end caps and Section 4 to the proposed upgrade of the vertex detector. Considerations of time table and cost are given in Section 5. The main points submitted for approval by the SPS Committee are summarized in the conclusions.

2. GENERAL CONSIDERATIONS

The experience gained in running UA2 at the Sp$\bar{p}$S collider has been decisive in the design of the upgraded detector.

The emphasis placed in the present design [11,12,13,14] on high mass final states containing parton jets, electrons and neutrinos has proven to be an excellent choice, mostly because of the low transverse momentum usually given to spectator particles (not directly involved in the short distance collision of interest). As a result of the high quality of the UA2 calorimetry (fine segmentation, tower geometry) we were able to give the first evidence for jet production at the Collider, for a resolved $Z^0 \rightarrow e^+e^-\gamma$ decay and for unexpected final states of the type discussed in Ref. 9. The absence of magnetic field in the central region was an essential factor in keeping the cost of UA2 nearly three times below that of UA1. It turned out to be a good choice since it does not significantly deteriorate the electron identification power as soon as the electron transverse momentum exceeds $\simeq$ 25 GeV/c and does not preclude competitive performance on the major physics issues. Similarly, the lack of muon detection, dictated by the desire to avoid the use of bulky equipment, such as thick absorbers and large magnetic field volumes, does not substantially impair the physics output of the UA2 detector. It is true that the restriction of lepton detection to electrons and neutrinos precludes their observation amid jet fragments, while significantly better results might be achieved with muons. This, however, has not yet been proven.

We do not propose, therefore, to alter the major design options of the present UA2 detector but rather to improve its performance in the domains where it is already effective : the detection of electrons, neutrinos and hadron jets.

The importance of a good missing transverse energy detection capability was not fully recognised when UA2 was designed in 1978. It now appears essential, not only to study final states containing an electron-neutrino pair, but also to search for possible supersymmetric particles, ultimately expected to decay into undetected photinos. Dead regions, such as the magnet coils of the forward UA2 spectrometers, and the lack of coverage below 20°, preclude an accurate missing transverse energy measurement. For example a two-jet event having a mass of $\simeq$ 50 GeV/c^2 is detected as a single jet event in $\simeq$ 2% of the cases, the other jet escaping detection.

The solid angle over which a hermetic coverage is necessary depends upon the mass range to be explored : a Monte Carlo study (see Section 3) indicates that a coverage down to $\simeq$ 10° from the beam line should be adequate. We propose therefore to extend down to this angle the transverse energy flow measurement presently performed in the central calorimeter, by replacing the forward spectrometers with segmented calorimeter end caps. In doing so we shall lose the ability to measure particle charges in this region but we consider the gain of improving on neutrino detection to be more important.

The early discoveries of the $W^{\pm}$ and Z^0 bosons through their eν and e^+e^- decay modes illustrate well the power of electron identification as a means of selecting interesting events among the bulk of hadronic collisions. In the present UA2 detector, jets can fake electrons at a level of the order of 10^{-5} of the inclusive jet yield. While this background is much lower than the electron signal from W and Z^0 decays, it is higher than the expected signal from semileptonic decays of t-quarks ($m(t) < 40$ GeV) by about one order of magnitude. In practice, because of lepton number conservation, an electron in the final state is expected to be associated with another electron of opposite sign or with a neutrino, and the presence of this second lepton provides further rejection against background. However, in the lower mass range, where both leptons have small transverse momenta, the background conditions are particularly difficult and any increase of the rejection factor against jets would substantially improve the detector performance. In the present detector the use of preshower counters contributes a factor of $\cong 10$ to this rejection factor. An improvement over the present situation implies a simultaneous discrimination against the two major types of misidentified electrons : converted photons from π^0 decays and unresolved π^0-$\pi^{\pm}$ pairs. In Section 4 we propose modifications to the UA2 vertex detector which will improve the situation. However, the spherical geometry of the present central calorimeter confines the cylindrical tracking detector to a maximum radius of 38 cm, imposing severe constraints on its design. In particular it precludes the use of transition radiation detectors, which could increase the rejection power against hadrons by two orders of magnitude. For this reason we considered the possibility to completely rebuild the central calorimeter with a cylindrical geometry allowing for a 1 metre radius volume available for both tracking and transition radiation detectors. However, having failed to find significant resources in manpower and money, we became convinced that such a project could not be achieved in time for 1987 and we decided to retain the present central calorimeter without modification. In doing so we deliberately give up the possibility of achieving spectacular improvements not only of the electron identification power but also of the hadronic energy resolution. The latter could in principle be improved by nearly a factor of 2 if uranium were used as converter material rather than iron and lead, together with a sampling material more uniform than scintillator. Such an improvement would substantially increase the ability of the detector to reveal possible structures in the mass distribution of multi-jet systems.

Our choice has been dictated by our conviction that the first two years of ACOL operation will be determinant to the success of the Sp$\bar{p}$S collider. We consider the Tevatron programme at Fermilab a very important constraint to our plans. This facility is scheduled to have its first physics run in 1986, and it is likely that by 1988 it will be fully operational with a luminosity similar to that of the CERN collider, and a centre-of-mass energy more than three times larger. It is therefore crucial to be ready for the 1987 run in order to compete efficiently with the Fermilab collider. We also consider that the simultaneous presence of two competitive experiments at the Sp$\bar{p}$S collider has been an essential factor of success. It has been efficient both at generating stimulation and at ensuring reliability. In designing the upgraded detector we have kept in mind these considerations and we took as essential that the competitivity of UA2 on the major physics issues be guaranteed as soon as the improved Sp$\bar{p}$S collider resumes operation in 1987.

3. CALORIMETER END CAPS

3.1 Introduction

In order to implement the transverse energy flow measurement down to small angles we propose to replace the present forward spectrometers with segmented calorimeter end caps. This approximately triples the longitudinal phase space coverage of the present central calorimeter and improves accordingly the ability of our apparatus to detect hadron jets and to provide an accurate measurement of missing transverse energy. The design provides for electron identification down to $\simeq 20°$ with a rejection power against background similar to that achieved in the central region.

We have studied the expected performance in relation to the measurement of transverse energy by simulating with a Monte Carlo programme the response of the detector to a set of two-jet events generated with ISAJET [15]. The detector coverage extends over a range of polar angles between θ_m and $180° - \theta_m$. Figure 1 shows the dependence upon θ_m of the average missing transverse energy under the assumption that one of the two jets has $p_\perp^{jet} > 25$ GeV/c and $20° < \theta_{jet} < 160°$. Figure 2 shows the distribution of the fraction of events having a missing transverse energy in excess of 20 GeV, f_{20}. A contribution of $\simeq 10^{-3}$, from events containing semi leptonic decays of heavy flavours, remains in the case of an "ideal" detector ($\theta_m = 0$, no energy measurement errors but no muon nor neutrino detection). For a realistic detector f_{20} levels off at $\simeq 10^{-2}$ for any $\theta_m < 10°$, one order of magnitude lower than in the present design. The results shown in Figures 1 and 2 are illustrative of the performance expected in the kinematical domain of practical interest and suggest to extend the end cap coverage down to $\theta_m \simeq 10°$. This implies the instrumentation of the forward cones down to $\theta_m \simeq 5°$ to allow for a reasonable margin around the actual fiducial volume.

3.2 End cap design

The proposed design is illustrated in Figures 3 to 5. A summary of the various end cap parameters is given in Table 1. Each end cap consists of 24 azimuthal sectors segmented in 9 cells (towers) pointing to the centre of the apparatus, each tower covering a same interval of pseudo-rapidity (except outside $-2.2 < \eta < 2.2$). The two cells at smaller polar angles have a larger azimuthal coverage (30° instead of 15°). Each cell is made of a 20 to 25 radiation length thick electromagnetic compartment using lead as converter and of a 5 to 6 absorption length thick hadronic compartment using iron as converter. The scintillator plates are made of extruded polystyrene and are read out via BBQ doped light guides housed at the interface of adjacent sectors. The converter plates extend over the full rapidity range of each azimuthal sector in order to minimize dead regions as well as for reasons of mechanical convenience. The sampling granularity (36 samplings in each electromagnetic compartment and 38 samplings in each hadronic compartment) should result in energy resolutions similar to those achieved in the central region.

The chosen geometry, vertical end caps normal to the beam line, preserves the possibility to replace the present central calorimeter at a later stage. A potential disadvantage of the proposed design is the presence of a discontinuity at $\theta = 40°$. We have studied in detail its influence on the transverse energy flow measurement with the help of a Monte Carlo simulation programme. The results, displayed in Figure 6, indicate that the effect is minor: in more than 90% of the cases the effect is limited to an interval of polar angle of about 5° and does not exceed 15%.

3.3 Electronics

The trigger and analog electronics associated with the new end caps are simple extensions of the system presently in use for the central calorimeter. We are discussing with the Saclay group to keep most of the components of the present forward calorimeters (phototubes, cables, ADC's, sample & hold's, etc...) in the new design.

3.4 Preshower counter

In the range of polar angle between 20° and 40° preshower counters located in front of the end cap electromagnetic compartments provide electron identification. They consist of a 2 r.l. lead converter followed by conductive plastic tube chambers with cathode strip readout. A schematic drawing of such a chamber is given in Figure 7. Eight slightly overlapping chambers in each of the forward and backward regions provide full azimuthal coverage. Similar chambers will be installed in front of the converter in order to get accurate space points on the charged particle tracks, close to the converter.

All strips and wires are equipped with analog readout. With a wire spacing and a strip pitch of ≅ 7mm the total number of signal channels for 32 chambers is about 12000. Multiplexing techniques will be used for the channel readout.

3.5 Calibration

Our experience with the present UA2 detector has shown how essential it is to devote a major effort to the initial calibration of the calorimeter cells and to thoroughly keep track of its evolution throughout the experiment. For that latter task we incorporate in the end cap design the same features as presently available in the central calorimeter with the addition of an improved scanning facility to measure the responses of both the electromagnetic and hadronic cells to a movable radioactive source. For what concerns test beam calibrations it is necessary to recalibrate the full central calorimeter in addition to the new end cap cells. These measurements can only take place in 1986 and their detailed implications on the availability of test beam time have been stated in a memorandum to the SPS Coordinator dated 27 February 1984. We should like to ask the SPS Committee to strongly support this request. We recall that for example the precision of the Z^0 mass determination depends directly on a good knowledge of the absolute energy scale. The currently best values are $m(Z^0) = 92.7 \pm 1.7 \pm 1.4$ GeV from UA2 [6] and $95.6 \pm 1.5 \pm 2.9$ GeV from UA1 [16], where the first error is statistical and the second error reflects the systematic uncertainty on the calibration of the electromagnetic calorimeter. The systematic uncertainty on the absolute energy scale of the hadronic calorimeter contributes in a significant way to the systematic error on the jet energy measurements.

The calibration procedure used for the UA2 central calorimeter is described in detail in Ref.11. The calibration relies on correcting the overall drifts (scintillators, BBQs, photomultipliers) using a light flasher system, measurements of the direct current induced by a ^{60}Co source and by measuring the average energy flow into each cell for unbiased $\bar{p}p$ collisions. It has been shown in Ref.11 that after a full calibration of all calorimeter modules in a beam the systematic uncertainty on the absolute energy scale can be kept, over several years, at ±1% (±2%) for the electromagnetic (hadronic) calorimeter with photomultiplier channel-to-channel rms spreads of 2% and 3% respectively.

4. UPGRADED VERTEX DETECTOR

4.1 Introduction

The present vertex detector (Fig.8) consists of two parts: a central tracking device, including four proportional chambers (C1 to 4) and two drift chambers (J1 to 2), and a preshower counter (C5). The proportional chambers are cylindrical with anode wires parallel to the beam line and with helical cathode strips. The drift chambers are segmented in 24 azimuthal cells, each cell containing six sense wires parallel to the beam. Charge division measurement is available on these wires. The detector recognises the pattern of tracks and measures their common vertex with a precision of 1mm in space. This feature is essential in the present design to allow for accurate momentum measurements in the forward spectrometers. Although this constraint is absent from the new design we must retain excellent tracking capability in order to cope with the increased luminosity which implies an occurence of multivertex events in about 1/3 of the cases. An essential role of the vertex detector is to provide an efficient and accurate measurement of electron tracks in order to evaluate the quality of their match with the associated preshower and calorimeter signals. This again implies a good tracking quality in order to retain a large, ambiguity-free reconstruction efficiency in the high multiplicity environment typical of high energy hadronic collisions. In order to improve the performance of the vertex detector along these lines, the upgraded design accomodates a much larger number of digitizations than presently available (Table 2).

Another task of the vertex detector is to provide an ionisation measurement for each individual track. We evaluate that about 1/3 of the presently misidentified electrons having a transverse momentum in excess of 15 GeV/c are in fact converted photons from π^0 decays (external conversions in the vacuum pipe or Dalitz pairs). The remaining 2/3 are associated with overlaps which have not been rejected by the preshower counter. The ionisation measurement is presently performed from the 12-fold sampling provided by the drift chambers. In the new design its quality is improved by equipping the chamber wires with flash ADC's allowing for a better two-track separation. In addition the insertion of a mosaic of silicon counters provides an independent ionisation measurement.

The proposed design is illustrated in Figure 9. It retains those parts of the present detector which can accomodate higher track densities without major modifications (C3 and 4, J1 and 2) and replaces the other parts by elements providing a significantly better granularity. Surrounding the 80mm diameter beryllium vacuum chamber, we find in order of increasing radii:

i) Four proportional chambers, A1 to A4.

ii) An array of silicon counters.

iii) The present stack of J1, C3, J2 and C4 with some modifications.

iv) The preshower counter.

4.2 The annular cathode chambers, A1 to A4

The present system of small diameter chambers, C1 to 2, suffers from an insufficient number of channels resulting in too high a strip occupancy in very high multiplicity events. We take advantage of the space made available by the replacement of the present vacuum chamber with one of smaller diameter to equip this region with a set of chambers offering a substantially higher granularity. While retaining the same general design of proportional chambers with cathode strip read-out, we choose a different geometry: four chambers instead of two in order to ensure adequate redundancy, and annular rather than helical cathode strips. This latter choice provides a direct visualisation of the track pattern in the r-z plane. Each strip is split in two semicircular parts to increase the number of available channels. This procedure is limited by the maximum permissible packing density of the lines bringing the signals to the chamber ends. In addition to their important role in helping the track pattern recognition, these chambers are essential to provide an early observation of electron tracks, prior to the ionisation measurement, in order to recognise photons converting inside the silicon array.

4.3 The silicon counter array

It is proposed to construct a matrix of 432 silicon detectors in a cylindre of 29cm diameter around the beam pipe and so provide, with good granularity, an ionisation measurement of charged tracks in the range $20° < \theta < 160°$ of polar angle. We aim at installation before the 1985 data taking period. Figure 10 shows the detector layout. Eighteen detectors ($6 \times 4 \times 0.03\ cm^3$) are arranged on each of 24 fiberglass boards covering an azimuthal interval of 15°. By overlapping individual detectors, the array has a negligible inactive area. Each detector is divided into 28 strips of area $\cong 0.9\ cm^2$. This preserves the future possibility of improving the granularity by using VLSI techniques of amplification and readout [17]. In 1985 it is intended to group sets of four strips into seven individual channels per detector, each of area $\cong 3.5\ cm^2$ (a total of 3024 channels). Hybrid preamplifiers will be mounted on the fiberglass board behind each detector. An array of three detectors will be tested in the UA2 apparatus during the 1984 run to reproduce all aspects of the proposed design.

To demonstrate the feasibility of this design, extensive prototype tests are in progress:

i) Pulse height resolution

Figure 11 shows the pulse height distribution for a Ruthenium β source in front of a $6\ cm^2$ counter simulated by connecting in parallel six independent counters of $1\ cm^2$ area each (noise is expected to be proportional to capacity). Tests are underway to demonstrate if satisfactory performance can be maintained when seven counters are grouped in a single detector.

ii) Radiation damage

We have exposed counters in the SPS tunnel, to ≅ 30 times the radiation expected in a typical $p\bar{p}$ period. During normal running the integrated radiation dose is negligible; any degradation of counter performance will result from irradiation during machine development periods. Again with counters of 1 cm^2 area, it has been shown that satisfactory counter and preamplifier performance is maintained. Tests are underway to demonstrate if detectors of the final configuration behave satisfactorily.

4.4 Modifications to the J1/2, C3/4 system

The present stack of chambers J1,C3,J2,C4 is retained with some modifications. The helical strips of C3 and C4 are cut in the centre thus dividing by two the average strip occupancy. The electronics of C1 and C2 are used to equip them. The jet chamber electronics are modified to incorporate a preamplifier/flash ADC system following recent developments achieved by the OPAL Collaboration [18]. In the jet chambers the two-track azimuthal resolving power is presently limited to ≅ 8mm due to the dead time of the multihit electronics. Using flash ADCs this resolving power can be improved by a factor ≅ 3. The OPAL studies have shown that the accuracy of the charge division measurement is kept below $\sigma(z)/L_{wire} \cong 1\%$, the same value as presently achieved in UA2.

4.5 The preshower counter

In the central region the preshower counter presently in use consists of a 1.5 r.l. tungsten converter followed by a proportional chamber equipped with helical cathode strips. The accuracy with which the signal position can be located on the chamber surface is ≅ ±3mm and the two-track resolving power is ≅ 20mm. By requiring a charge equivalent to three times the average charge deposited by a minimum ionising particle, an efficiency of ≅ 95% is obtained. In the proposed design the new preshower counter aims at making up for two limitations of the existing chamber: the possible confusion in high π^0 multiplicity environment resulting from the ambiguities of space point reconstruction, and the lack of redundancy in case of a local failure. In addition it provides significant improvement to the accuracy of the measurement of the track-cluster match.

5. TIME TABLE, MANPOWER AND COST

We have analysed the various operations implied in the construction, testing and assembly of the proposed upgraded design and we have found that the overall time table is governed by the operations associated with the end cap calorimeters. Table 3 gives a summary of the main milestones. The margin between the end of the assembly and testing operations and the start of the Autumn 1987 run barely exceeds two months.

A cost analysis of the various parts of the proposed upgraded design has been made. A summary is given in Table 4. The overall cost is ≅ 6 MSF, two thirds of which are associated with the new end caps.

In addition to the Institutes which have been involved in the construction of UA2 (with the exception of Copenhagen and Saclay) a new group from Pisa joins in the proposed effort. We are having contacts with a number of other groups (among which Cambridge and Rutherford) in order to further enlarge the present Collaboration and to achieve a better distribution of effort and resources. While we have made sure that the manpower necessary to the implementation of the present proposal is available among its signees, new collaborators would be encouraged.

6. CONCLUSIONS

We propose a set of modifications to the present UA2 detector with the aim to match its performance to that of the improved Sp$\bar{p}$S Collider.

The proposed design results from a number of choices dictated by the following considerations:

i) The upgraded UA2 must be operational in 1987, as soon as the Collider resumes operation, in order to maximise its physics output during the period when TEV 1, with nearly three times as high a c.m. energy, has not yet taken over leadership.

ii) The upgraded UA2 must remain competitive on the major physics issues rather than diversify its detection capabilities.

iii) Priority is given to the quality of the missing transverse energy measurement.

iv) Modifications to the vertex detector aim at ensuring that multivertex events can be reconstructed and at improving the detector performance in relation with electron identification.

We request the SPS Committee to give their approval to the above choices and to the general lines of the proposed design in order for us to start working on its implementation without delay.

We should like, however, to retain the freedom of possibly making some changes to the proposed design to the extent that they do not introduce delay nor increase substantially the overall cost. Such a flexibility is particularly appropriate for new groups joining the proposed effort. Our approach, as it is presented in this document, is rather conservative in that most of the proposed modifications require no development effort. However, we are presently planning or performing feasibility studies of less conventional solutions. These include in particular a compact vertex detector made of scintillating fibers, following the work of the Cambridge group and leaving sufficient clearance to accomodate a transition radiation detector. They also include a silicon strip preshower detector in the central region for better electron identification by improved charge localisation. A prototype module will be tested later this year.

If such modifications to the present proposal are appropriate we shall report to the SPS Committee in due time.

REFERENCES

1. M. Banner et al., Phys. Lett. 118B (1982) 203.
2. P. Bagnaia et al., CERN-EP/84-12.
3. P. Bagnaia et al., Z. Phys. C 20 (1983) 117.
4. UA2 Collaboration, CERN 83-04 (1983), p. 190.
5. M. Banner et al., Phys. Lett. 122B (1983) 476.
6. P. Bagnaia et al., CERN-EP/84-39.
7. P. Bagnaia et al., Phys. Lett. 129B (1983) 130.
8. G. Arnison et al., Phys. Lett. 135B (1984) 250.
9. P. Bagnaia et al., Phys. Lett. 139B (1984) 105.
10. G. Arnison et al., CERN-EP/84-42.
11. A. Beer et al., CERN-EP/83-175.
12. M. Dialinas et al., LAL-RT/83-14.
13. C. Conta et al., CERN-EP/83-176.
14. K. Borer et al., CERN-EP/83-177.
15. F.E. Paige and S.D. Protopescu, BNL-31987.
16. G. Arnison et al., Phys. Lett. 126B (1983) 398.
17. J.T. Walker , S. Parker, B. Hyams and S.L. Shapiro, Development of high density readout for silicon strip detectors, Proc. 3rd Eur. Conf. on semiconductor detectors, to be published in Nucl. Inst. Meth.

18. OPAL Technical Report, pp 58 and ff.

TABLE 1: End Cap Calorimeter

Electromagnetic calorimeter	
technique	Pb-scintillator sandwich BBQ read out
material	36 Pb plates, 3 mm thick 37 scintillator plates, 4 mm thick
sampling	0.54 to 0.70 X_0
total thickness	19.4 to 25.2 X_0
Hadronic calorimeter	
technique	Fe-scintillator sandwich BBQ read out
material	Fe plates, 25 mm thick scintillator plates, 5 mm thick $5^\circ < \theta < 20^\circ$ 38 plates each $20^\circ < \theta < 40^\circ$ staggered, with 29 plates each at $\theta \simeq 40^\circ$.
sampling	0.15 to 0.19 λ_0
total thickness	5.6 to 6.2 λ_0 (0.6 to 0.8 λ_0 in addition from the electromagnetic calorimeter)
segmentation	
structure	towers pointing to the centre of the detector
cell size	$1.0 < \lvert\eta\rvert < 2.2$: $\Delta\phi \times \Delta\eta = 15^\circ \times 0.2$ $2.2 < \lvert\eta\rvert < 2.5$: $\Delta\phi \times \Delta\eta = 30^\circ \times 0.3$ $2.5 < \lvert\eta\rvert < 3.0$: $\Delta\phi \times \Delta\eta = 30^\circ \times 0.5$
depth segmentation	one electromagnetic and one hadronic compartment
sector	30° in azimuth, 24 sectors in total
number of cells	electromagnetic 336 hadronic 384
number of channels	2 PM's per cell, 1440 total
approximate weight	
	120t for each end cap

The thicknesses in radiation length (X_0) and absorption length (λ_0) vary as a function of the polar angle θ between 5° and 40° with respect to the beam axis.

TABLE 2: Vertex Detector Chambers

Chamber	Radius (mm)	Length (mm)	Number of Wires	Number of Strips
C_4	315	1860	864	1344 (2 layers)
C_3	240	1600	576	1056 (2 layers)
A_4	118	1080	384	552 (1 layer)
A_3	96	1000	312	504 (1 layer)
A_2	74	920	240	456 (1 layer)
A_1	52	840	168	408 (1 layer)
J_2	∿ 270	1800	144	
J_1	∿ 210	1530	144	

Total No of wires

C_3 C_4	1440
Jet	288
A_1 A_4	1104

Total No of Strips

C_3 C_4	2400
A_1 A_4	1920

TABLE 3: Calorimeter End Caps, Time Table

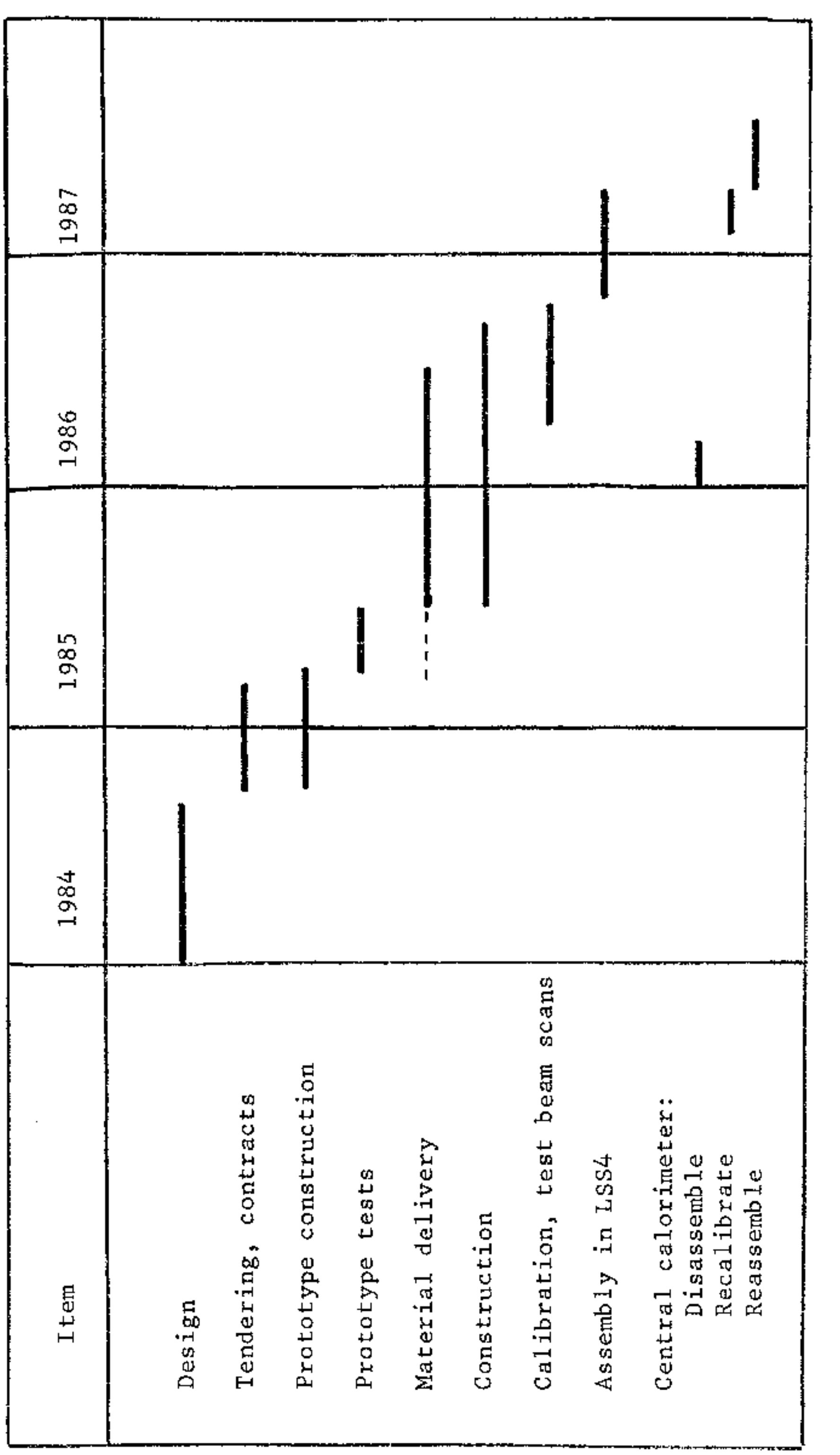

TABLE 4: Cost Summary (kSF)

End caps	
Calorimeter	
Mechanics	2500
Electronics	500
Manpower	500
Preshower	700
Vertex detector	
A1 to 4	250
Silicon matrix	500
J1 to 2, C3 to 4	350
Preshower	400
Miscellaneous	200
TOTAL	5900

FIGURE CAPTIONS

1. Average missing transverse energy as a function of polar angle coverage (θ_m to $180°-\theta_m$) for a sample of two-jet events generated using ISAJET [15].

   a) "ideal" detector (see text)

   b) proposed upgraded UA2 calorimeter

   c) present UA2 set-up. The cross-hatched area refers to the use of different algorithms in the forward regions.

2. Fraction of events with a missing transverse energy in excess of 20 GeV as a function of calorimeter coverage for the same event sample as in Figure 1 and for the same cases a), b) and c).

3. The UA2 central calorimeter and the proposed end cap calorimeter: schematic cross-section in a plane containing the beam line.

4. Schematic view of the front iron absorber plate of a sector of the end cap calorimeter, indicating the cell structure.

5. Perspective view of one of the two end cap calorimeters showing the front faces of the electromagnetic and hadronic calorimeters.

6. Central calorimeter / End cap interface

   a) typical longitudinal vertex distribution.

   b) definition of polar angle θ and vertex offset Δz.

   c) effect of the 40° discontinuity: the ratio between the detected and generated energies as a function of polar angle for a sample of Monte Carlo jets having 40 GeV transverse energy. The curves correspond to different values of the vertex offset Δz and are labelled with its value in mm. Vertical bars indicate rms deviations with respect to the mean.

7. Schematic drawing of an end cap preshower chamber.

8. Exploded view of the present vertex detector indicating schematically the arrangement of the various components.

9. Proposed arrangement of the vertex detector components in the proposed design.

10. Silicon array geometry

    a) overall schematic arrangement

    b) detail of the overlap scheme

    c) dimensions of a single counter

11. Measured response of a silicon counter. The distribution peaked at lower values (full circles) results from particles traversing one counter, the distribution peaked at higher values (open circles) results from particles traversing two counters.

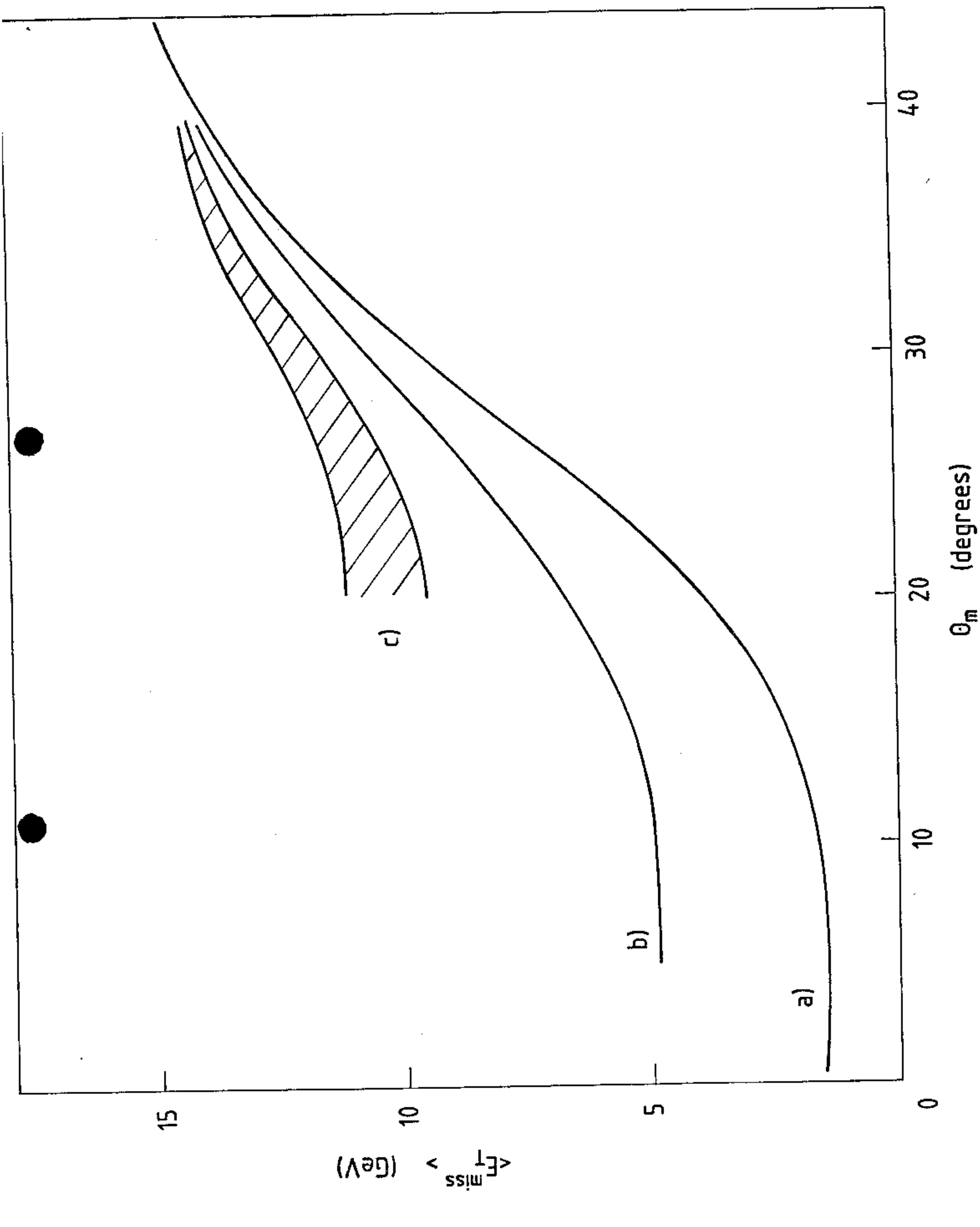

Figure 1

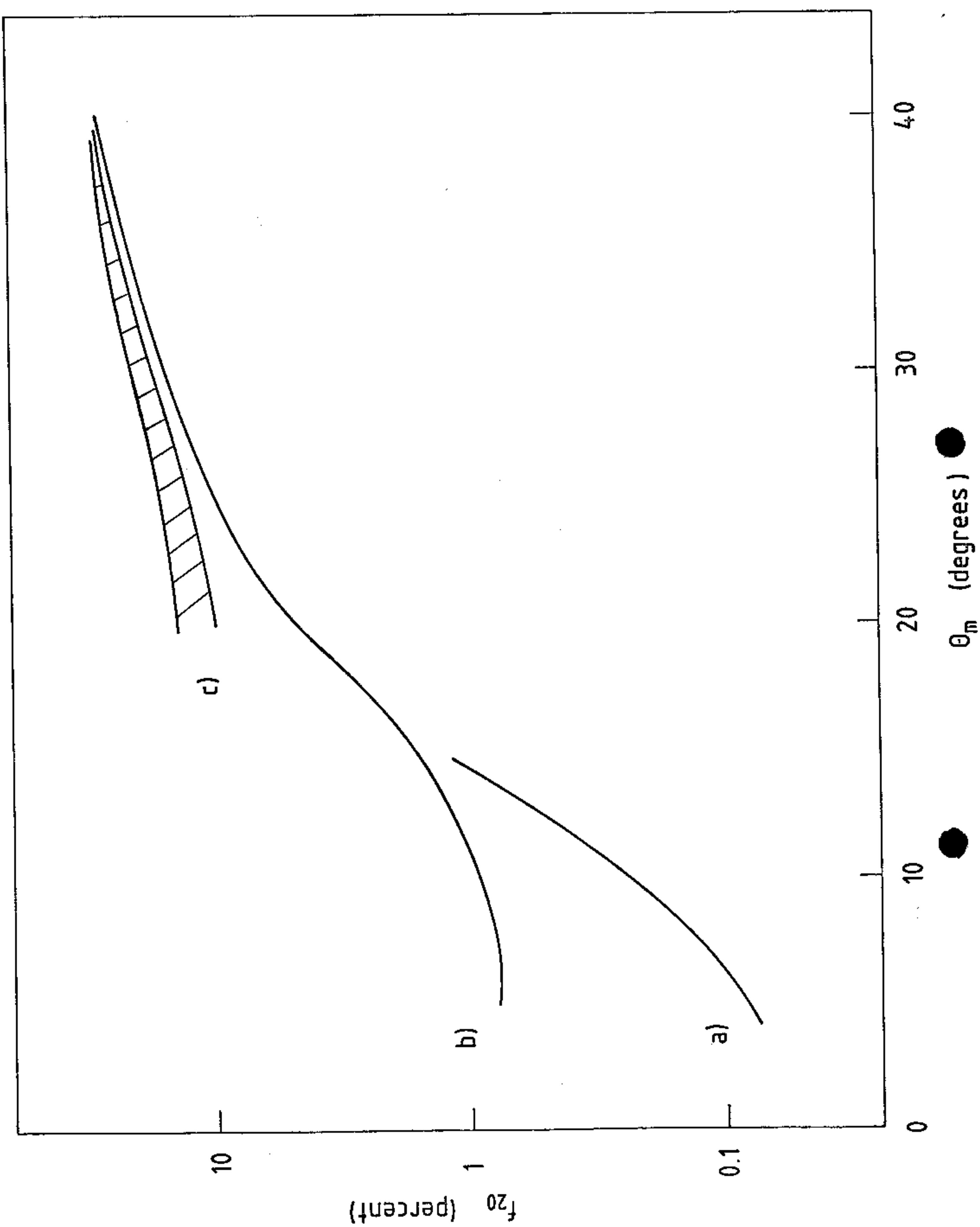

Figure 2

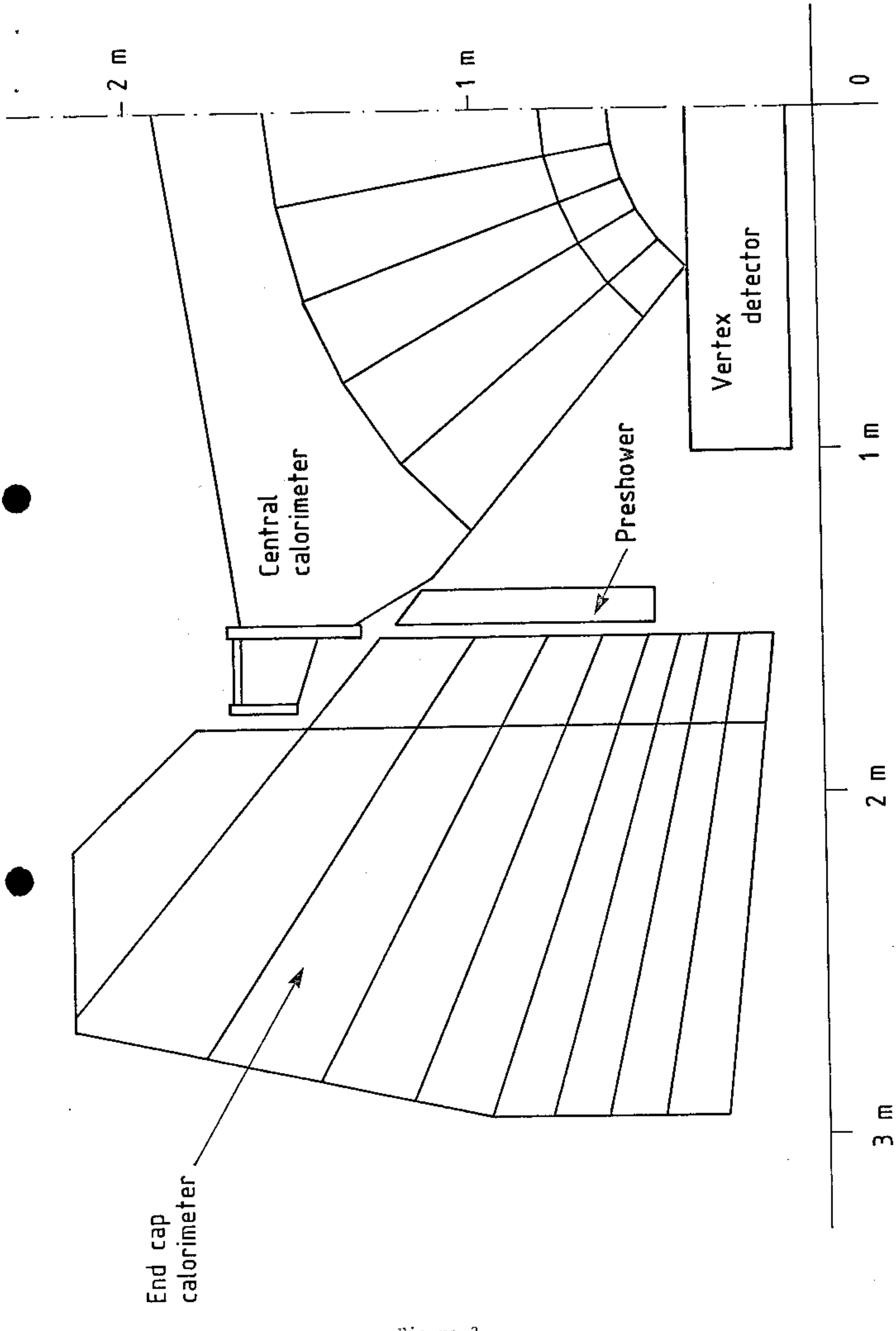
2 m
1 m
0
Vertex detector
Preshower
Central calorimeter
End cap calorimeter
1 m
2 m
3 m

Figure 3

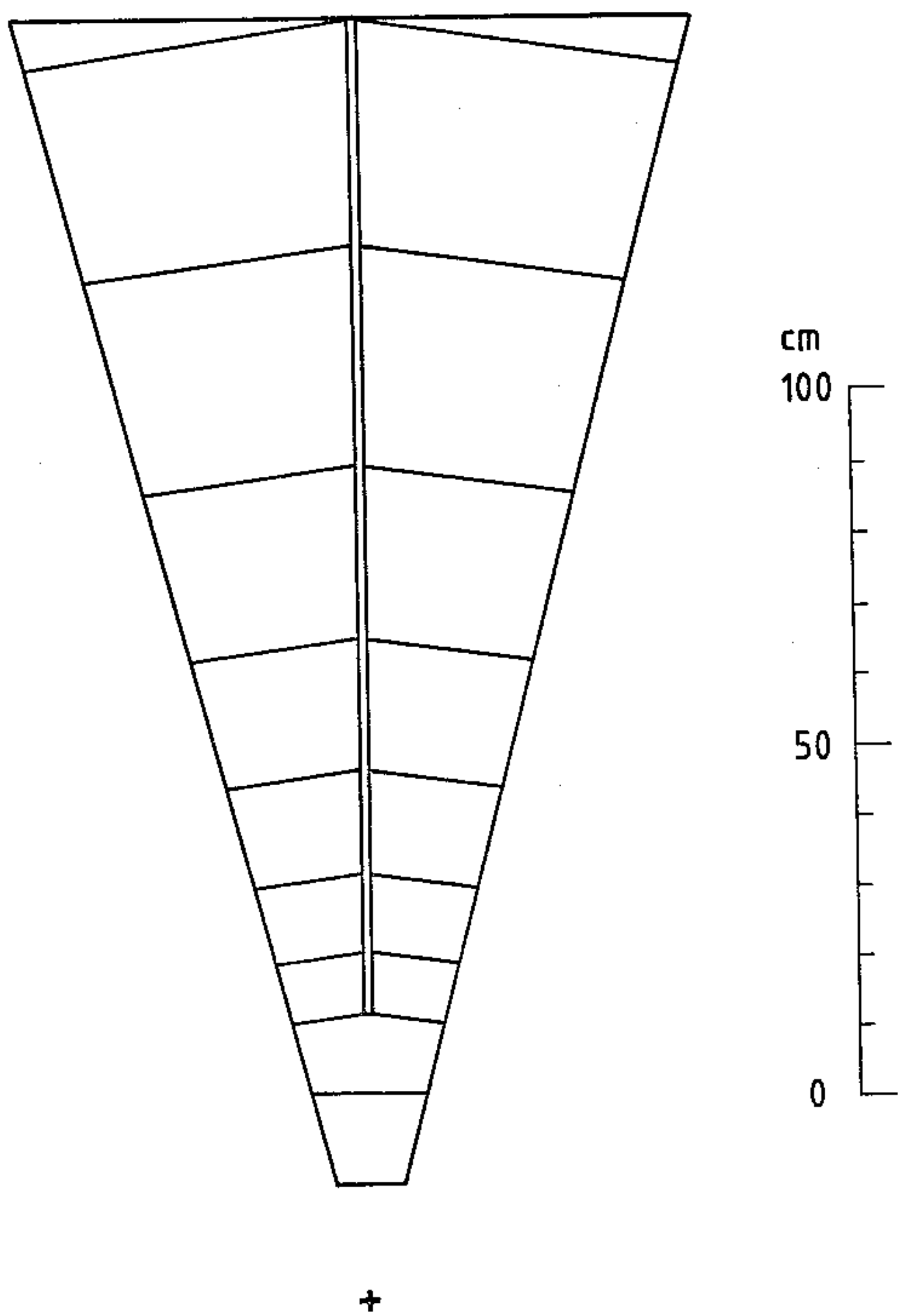

Figure 4

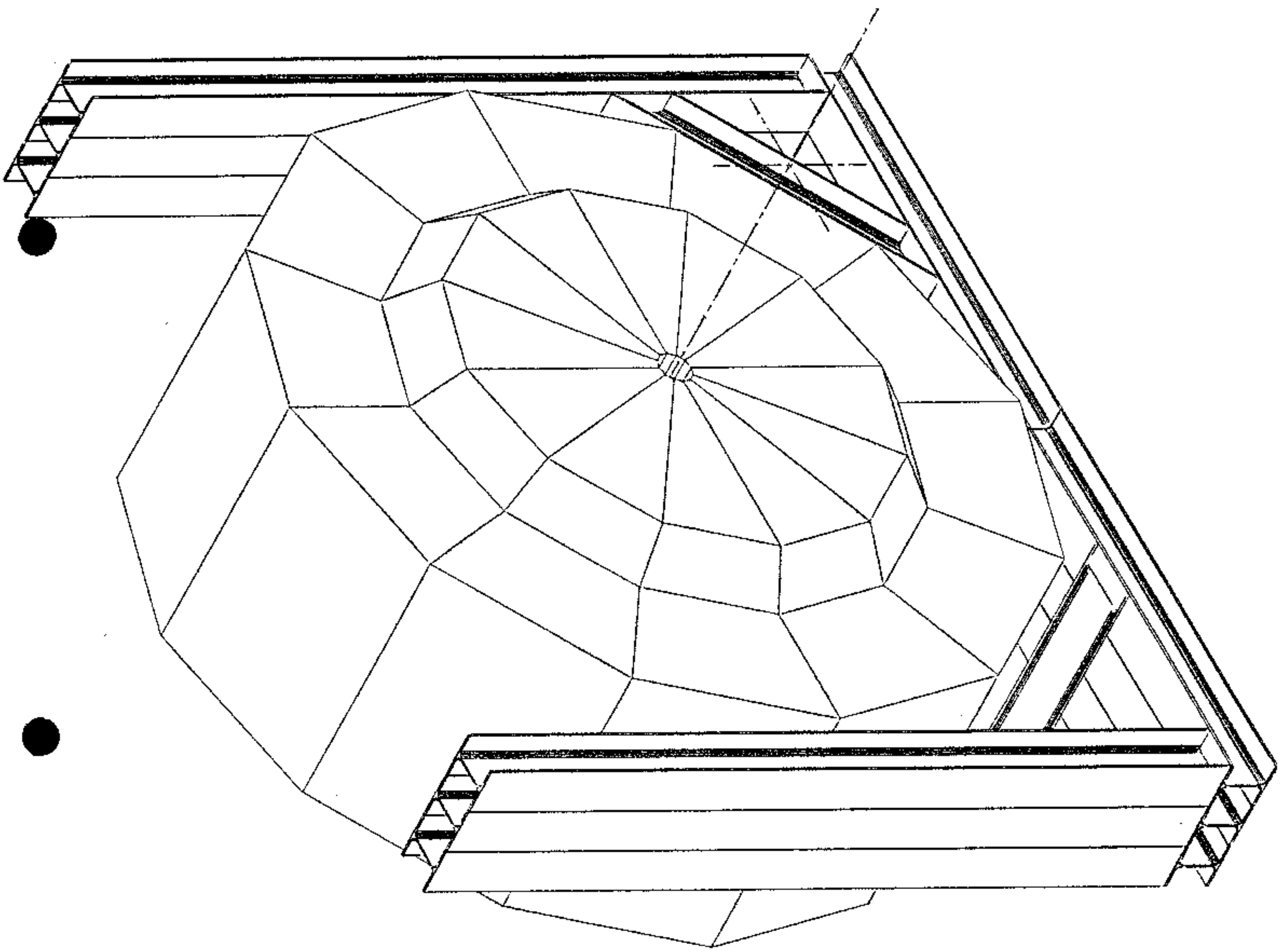

Figure 5

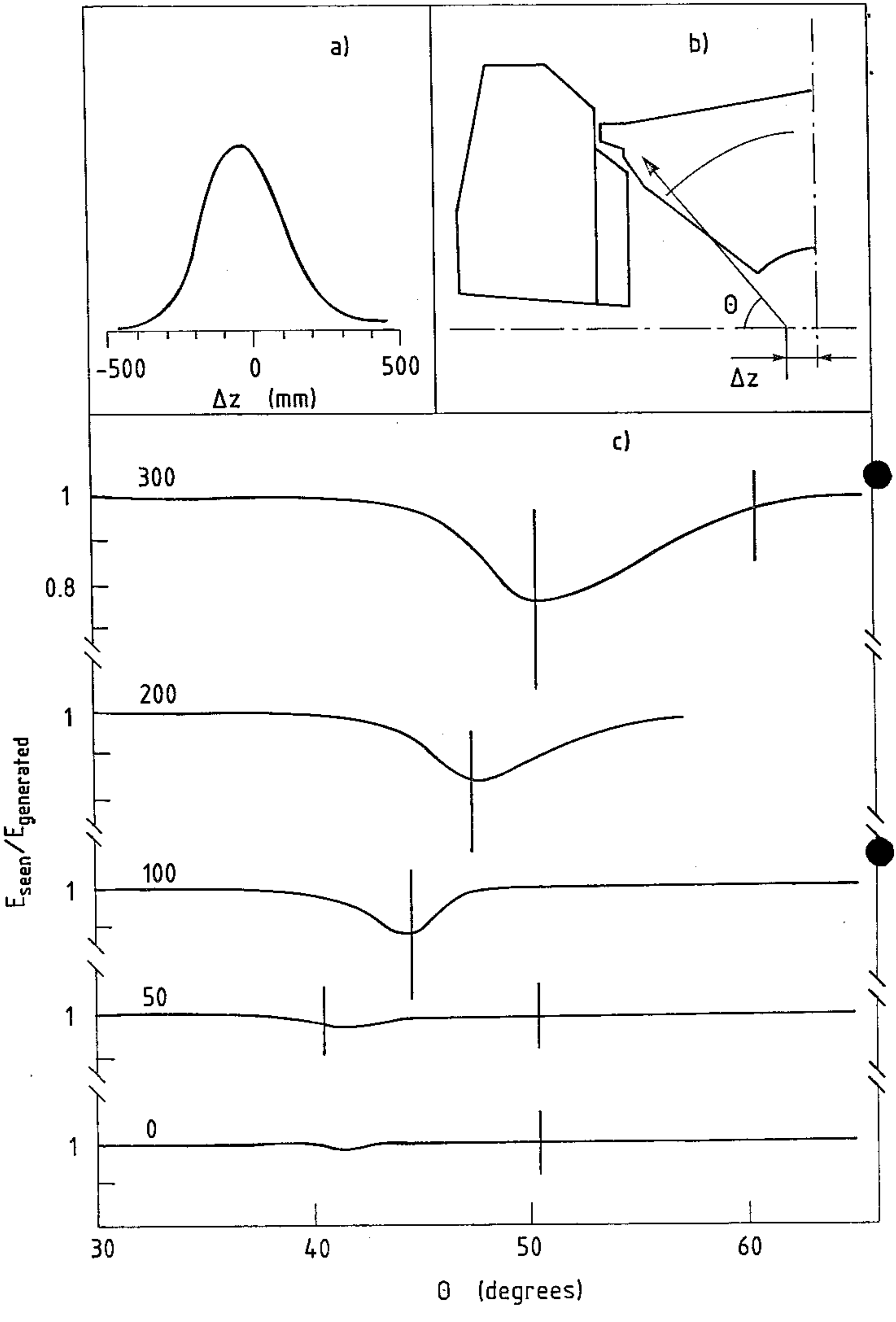
a)
-500
0
500
Δz (mm)
b)
Θ
Δz
c)
300
200
100
50
0
1
0.8
E_seen/E_generated
30
40
50
60
Θ (degrees)

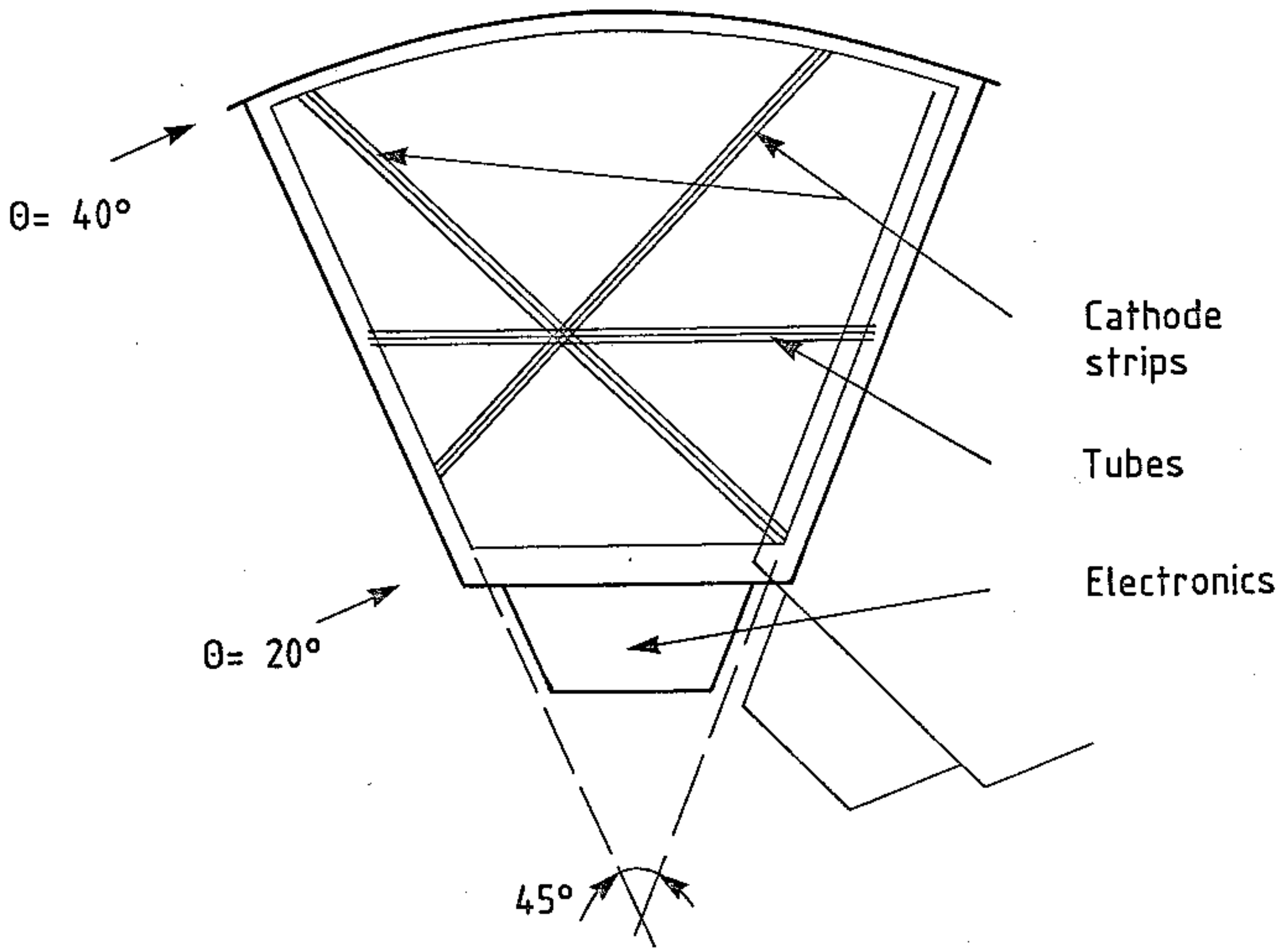

Figure 7

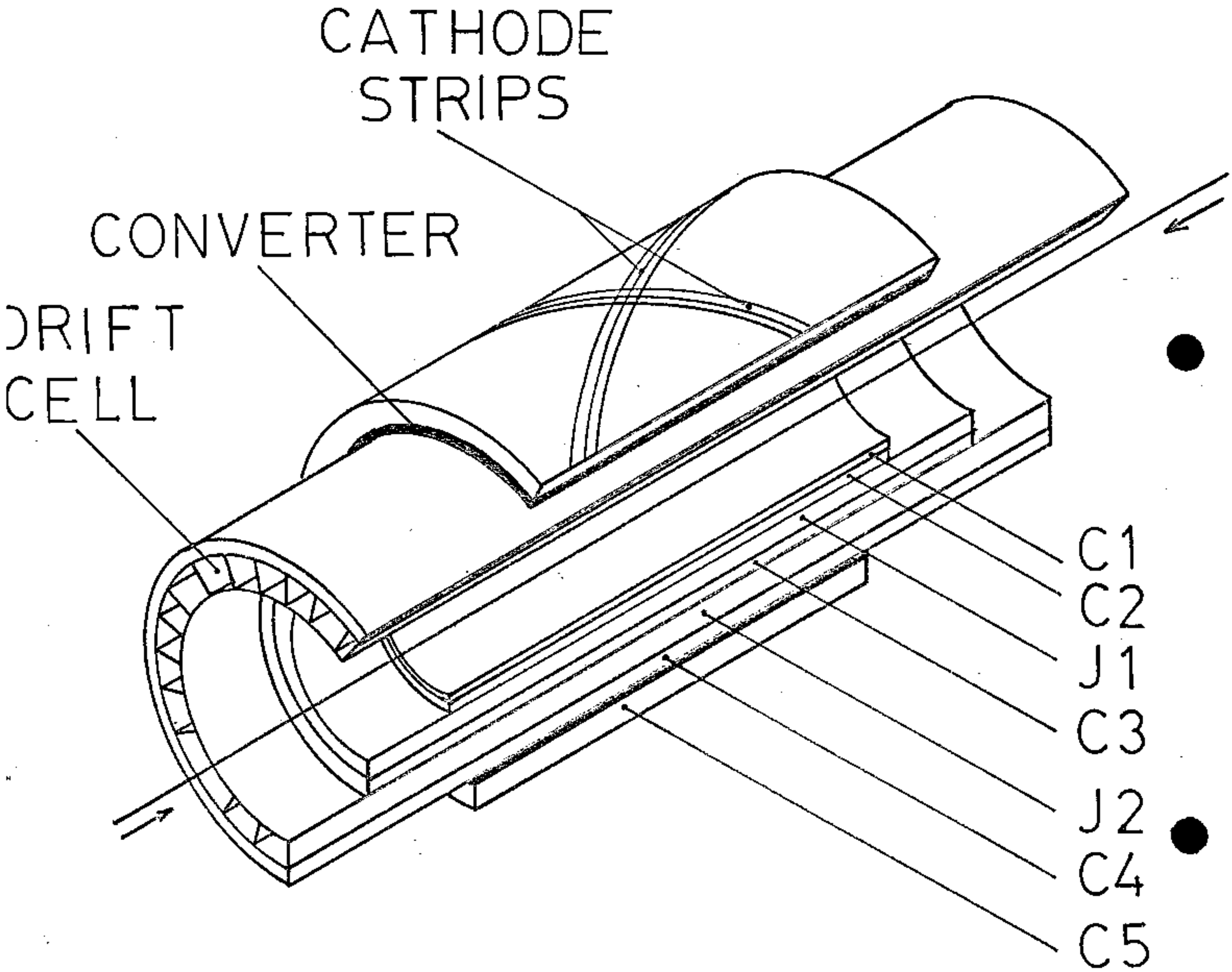

Figure 8

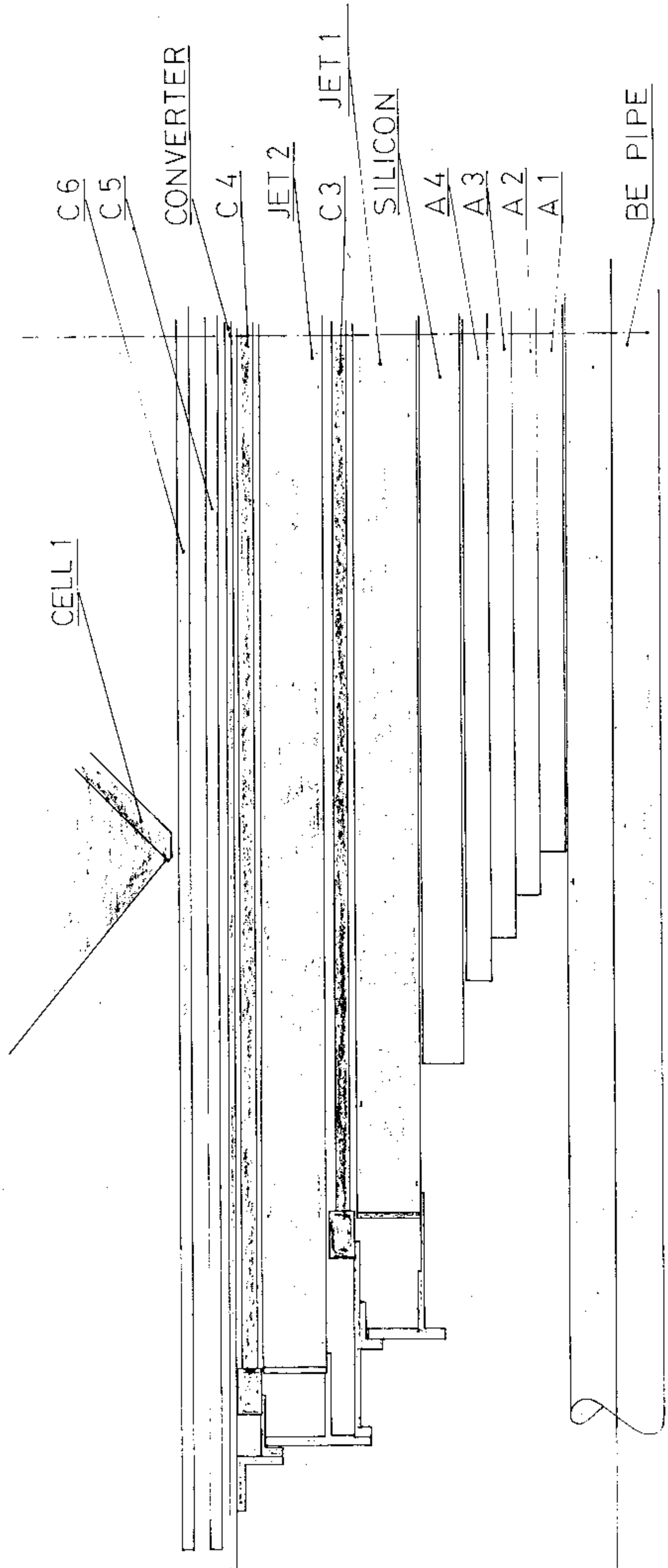
CELL 1
C 6
C 5
CONVERTER
C 4
JET 2
C 3
JET 1
SILICON
A 4
A 3
A 2
A 1
BE PIPE

Figure 9

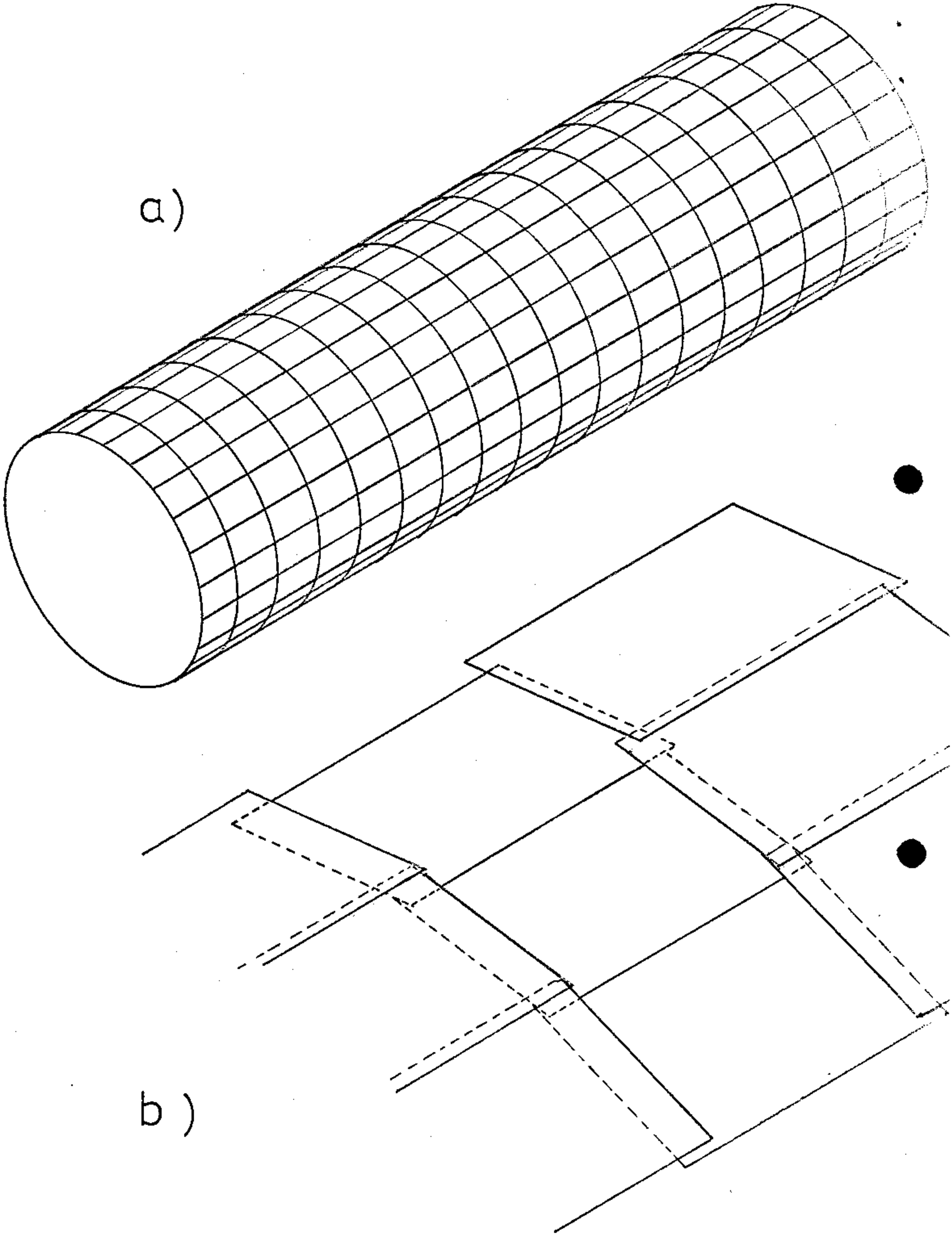

Figure 10

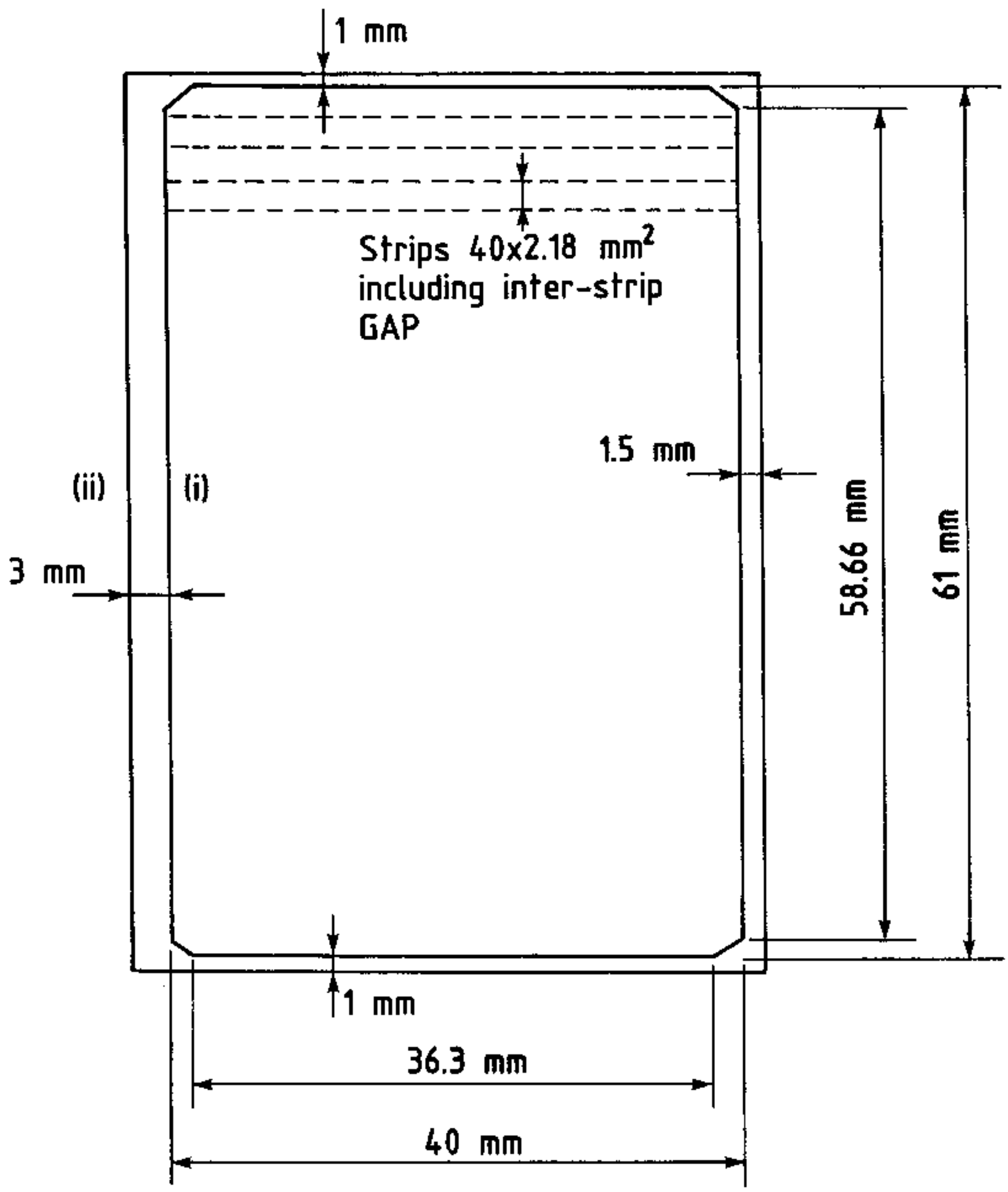
1 mm
Strips 40x2.18 mm²
including inter-strip
GAP
1.5 mm
(ii)
(i)
3 mm
58.66 mm
61 mm
1 mm
36.3 mm
40 mm

Figure 10c

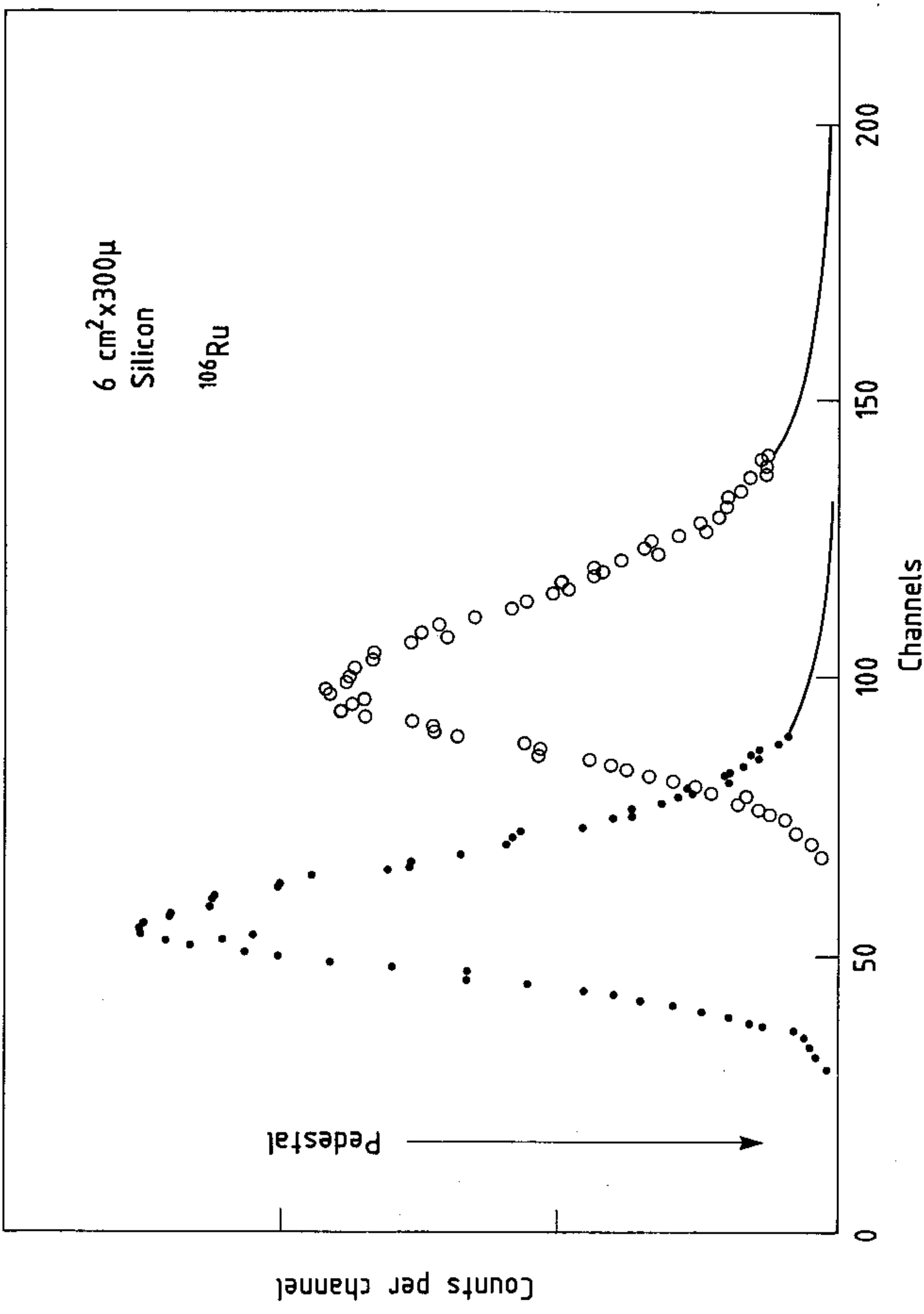

6 cm²x300μ
Silicon
106Ru
Pedestal
Counts per channel
Channels
0
50
100
150
200

Figure 11